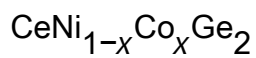


Thermal properties of various Kondo ground states in the heavy-fermion system



This article has been downloaded from IOPscience. Please scroll down to see the full text article.

2005 J. Phys.: Condens. Matter 17 2485

(<http://iopscience.iop.org/0953-8984/17/15/019>)

View [the table of contents for this issue](#), or go to the [journal homepage](#) for more

Download details:

IP Address: 129.252.86.83

The article was downloaded on 27/05/2010 at 20:38

Please note that [terms and conditions apply](#).

Thermal properties of various Kondo ground states in the heavy-fermion system $\text{CeNi}_{1-x}\text{Co}_x\text{Ge}_2$

J B Hong¹, Tuson Park² and Y S Kwon^{1,3,4}

¹ BK21 Physics Research Division and Institute of Basic Science, Sungkyunkwan University, Suwon 440-746, Korea

² Los Alamos National Laboratory, Los Alamos, NM 87545, USA

³ Center for Strongly Correlated Material Research, Seoul National University, Seoul 151-742, Korea

E-mail: yskwon@skku.ac.kr

Received 12 January 2005, in final form 2 March 2005

Published 1 April 2005

Online at stacks.iop.org/JPhysCM/17/2485

Abstract

We report results of the specific heat of the heavy-fermion compounds of the alloying series $\text{CeNi}_{1-x}\text{Co}_x\text{Ge}_2$. With increasing x , hybridization between the localized 4f and conduction band electrons is enhanced. The magnetic order observed for the $x = 0$ composition is completely suppressed at a critical concentration of $x_c = 0.3$, yielding Fermi-liquid behaviour for $x > 0.3$. We observe significant deviations from the Fermi-liquid behaviour at $x_c = 0.3$. Anomalies found in the specific heat are well explained by the Kondo model for a degenerate impurity spin $J = 1/2, 3/2$, and $5/2$ in the Coqblin–Schrieffer limit for the Co concentration ranges of $x \leq 0.6$, $0.7 \leq x \leq 0.8$, and $x \geq 0.9$, respectively.

1. Introduction

Ce-based ternary intermetallic compounds are the subject of continuous interest because of a wide variety of their ground states. These compounds have a localized 4f electron for each Ce^{3+} ion and exhibit the dense Kondo behaviour at high temperatures. Upon cooling, several magnetic ground states are realized through competition between Kondo and RKKY (Ruderman–Kittle–Kasuya–Yosida) energy scales [1, 2]. The formation of a local Kondo singlet depends exponentially on the exchange interaction J_0 , $T_K \propto \exp(-1/N_F J_0)$, while the formation of long-range magnetic order depends quadratically on J_0 , $T_{\text{RKKY}} \propto (N_F J_0)^2$ [2, 3], where $N_F J_0$ is a dimensionless effective exchange coupling constant for coupling between 4f localized magnetic moments and conduction electrons with the density of states N_F at the Fermi level. For a small value of $N_F J_0$ a local-moment magnetism (LMM) is dominant, while for a large value of $N_F J_0$ an intermediate-valence (IV) behaviour is anticipated. Just at the

⁴ Author to whom any correspondence should be addressed.

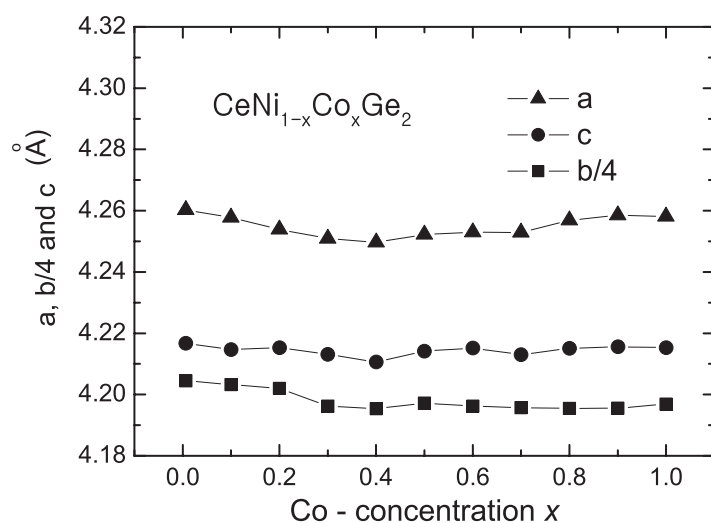


Figure 1. Lattice parameters a , b , and c versus Co concentration x . Here, b is plotted divided by four for better presentation.

borderline from the LMM regime to the IV regime, the heavy-fermion (HF) behaviour is often observed.

In the present study, we control the hybridization strength through changing isoelectronic chemical substitution. Then, the system is expected to pass through a quantum critical point at the boundary between the LMM and IV regimes. Here, we have paid special attention to the critical concentration where the magnetism of the undoped system is completely suppressed. For this investigation, we have chosen the ternary alloys of $\text{CeNi}_{1-x}\text{Co}_x\text{Ge}_2$ ($0 \leq x \leq 1$). CeNiGe_2 is a heavy-fermion local-moment system with a large Sommerfeld coefficient $\gamma = 97.6 \text{ mJ mol}^{-1} \text{ K}^{-2}$ [4], while CeNiSi_2 is a heavy-fermion valence fluctuating compound with $\gamma = 128 \text{ mJ mol}^{-1} \text{ K}^{-2}$ [5]. Recently it was found by us that CeCoGe_2 is a nonmagnetic heavy-fermion Kondo compound with $J = 5/2$ ground state with the Kondo temperature $T_K > 200 \text{ K}$ [6]. Although preliminary results of magnetic susceptibility and resistivity have been previously reported [7], in this paper we present a experimental report together with a theoretical analysis of the thermal properties of the $\text{CeNi}_{1-x}\text{Co}_x\text{Ge}_2$ system.

2. Experimental details

We used starting materials of high purity: lanthanum and cerium (99.9 at.% pure), cobalt and nickel (99.95 at.% pure) and germanium (99.999 at.% pure). Polycrystalline samples of $\text{CeNi}_{1-x}\text{Co}_x\text{Ge}_2$ ($0 \leq x \leq 1$) were prepared by arc melting under argon atmosphere and then annealed at 900°C for three weeks inside an evacuated quartz tube. Less than 0.3% weight loss occurred during the melting process. Metallographic analysis indicated that the samples used in this study were essentially single phase. The powder x-ray diffraction pattern revealed that they crystallize in the orthorhombic CeNiSi_2 -type (space group $Cmcm$) structure. For the whole concentration, the lattice parameters of a , b , and c remain almost unchanged (see figure 1). Even in the region of $x < 0.3$, where the lattice parameters are slightly decreased with increasing x , the change of volume ratio $[V(x) - V(x = 1)]/V(x = 1)$ is less than 0.5%. For comparison, about 10% change of volume was observed for other alloys such as

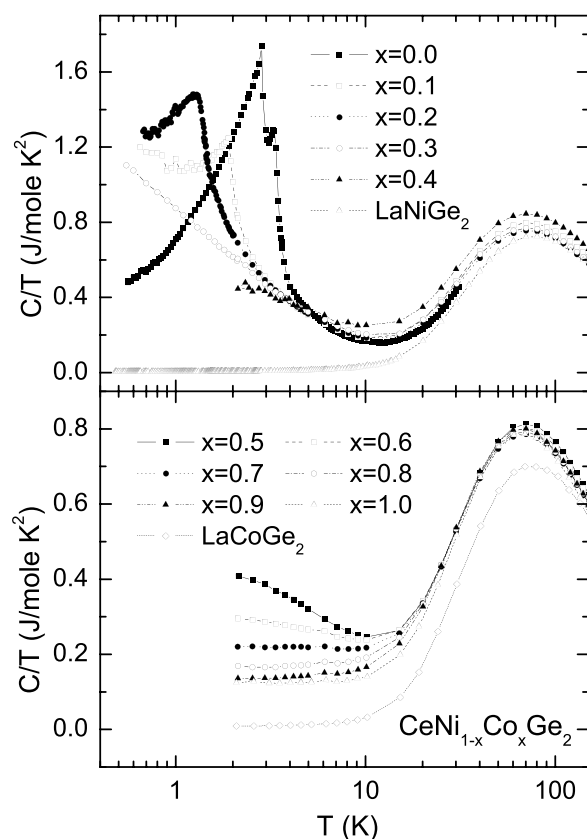


Figure 2. Specific heat divided by temperature C/T for $\text{CeNi}_{1-x}\text{Co}_x\text{Ge}_2$ as well as LaNiGe_2 and LaCoGe_2 .

$\text{Ce}(\text{Pd}_{1-x}\text{Ni}_x)_2\text{Ge}_2$ [8], $\text{CeNi}_2(\text{Ge}_{1-x}\text{Si}_x)_2$ [8], $\text{CeCu}_{2-x}\text{Ni}_x\text{Si}_2$ [9], and $\text{CeCu}_{6-x}\text{Au}_x$ [11]. This result implies that in our system of $\text{CeNi}_{1-x}\text{Co}_x\text{Ge}_2$ the crystallographic distortion due to the substitution, i.e. chemical pressure effect, is nearly negligible. Thus, we believe that the change of physical properties in $\text{CeNi}_{1-x}\text{Co}_x\text{Ge}_2$ is most likely to arise from the difference of electron density between Ni and Co ions. The specific heat data were taken by a relaxation method with a Quantum Design physical property measurement system (PPMS9) from 2 to 150 K. The specific heat below 2 K was measured by an adiabatic method using a home-made ^3He refrigerator.

3. Experimental results and analysis

Figure 2 shows C/T of $\text{CeNi}_{1-x}\text{Co}_x\text{Ge}_2$ between 0.5 and 150 K on a semi-log scale. At $x = 0$, two peaks are observed at 3.40 and 2.84 K, which correspond to the two-step antiferromagnetic transitions as reported earlier [7, 10]. With increasing x , the two peaks are merged into one, i.e., to 1.95 K at $x = 0.1$. On further increasing x , no anomaly is found down to 0.5 K, indicating that the antiferromagnetic transition temperature is suppressed to zero near $x = 0.3$. Sommerfeld coefficient γ was estimated from the low-temperature C/T . As shown in figure 3, the linear specific heat coefficient is large for the whole concentration range, but strongly depends on

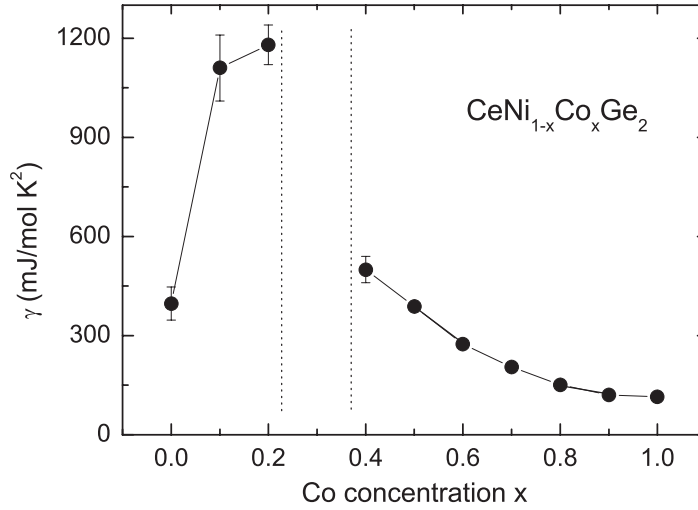


Figure 3. Sommerfeld coefficient γ as a function of Co concentration x in $\text{CeNi}_{1-x}\text{Co}_x\text{Ge}_2$.

the Co concentration. It rapidly increases with increasing x for $x < 0.3$, while it gradually decreases with x for $x > 0.3$. At $x = 0.3$, γ diverges and C/T follows $-\ln T$ dependence below 6 K. This logarithmic temperature dependence of C/T , which is a characteristic feature of non-Fermi-liquid phenomena, strongly suggests that $x = 0.3$ is a quantum critical point.

Figure 4 shows the magnetic specific heat, i.e., $C_{4f} = C(\text{CeNi}_{1-x}\text{Co}_x\text{Ge}_2) - C(\text{LaNi}_{1-x}\text{Co}_x\text{Ge}_2)$, where the specific heat of the nonmagnetic counterpart, $\text{LaNi}_{1-x}\text{Co}_x\text{Ge}_2$, was subtracted. For $0.4 \leq x \leq 1$, C_{4f} exhibits a broad peak, which moves toward lower temperature with decreasing x . The broad peak at $x = 1$ can be explained by the Coqblin–Schrieffer (CS) model with $j = 5/2$ and $T_0 = 220$ K (see the top panel of figure 4) [6, 12, 14], suggesting that the crystalline-electric-field (CEF) splitting is negligible compared to large Kondo fluctuations. For $0.7 \leq x \leq 0.9$, the experimental data are smaller than the result calculated by the CS model for $j = 5/2$ but are larger than that for $j = 3/2$ (see the top panel of figure 4), indicating that the CEF splitting is comparable to the Kondo temperature. The numerical solution for a degenerate Kondo model, where the $j = 5/2$ multiplet splits into three equally spaced doublets separated by an energy Δ , has been reported by Desgranges *et al* [13]. Although the CEF splitting scheme applied in their model may be different from ours, where the splitting energies may be unequal, the difference can be ignored if $\Delta/T_K < 0.5$. Figure 5 compares the experimental data and the numerical calculation (solid curves) based on the CS model with the equally spaced CEF splitting [13]. Best results were obtained with the following parameters: $\Delta/T_K = 0.3$ and $T_K = 193$ K for $x = 0.9$, $\Delta/T_K = 0.47$ and $T_K = 148$ K for $x = 0.8$, and $\Delta/T_K = 0.53$ and $T_K = 120$ K for $x = 0.7$. These results suggest that the Kondo temperature at $x = 0.9$ is larger than the crystal field splitting energy ($2\Delta = 116$ K) but the T_K values at $x = 0.8$ and 0.7 are of same order as or slightly smaller than the 2Δ .

For $0.4 \leq x \leq 0.6$ (see the middle panel of figure 4), the Kondo solution mentioned above cannot be applied because Δ/T_K is expected to be larger than 0.5. When we apply the $j = 3/2$ degenerate Kondo result calculated by Rajan [14], our data are lower than the calculated values at the broad peak temperature (40 K), while they are higher than the calculated values at the shoulder near 10 K. We conjecture that the broad peak is related to CEF effects, while the shoulder is due to the $j = 1/2$ Kondo state. In the middle right panel of figure 5, we show the

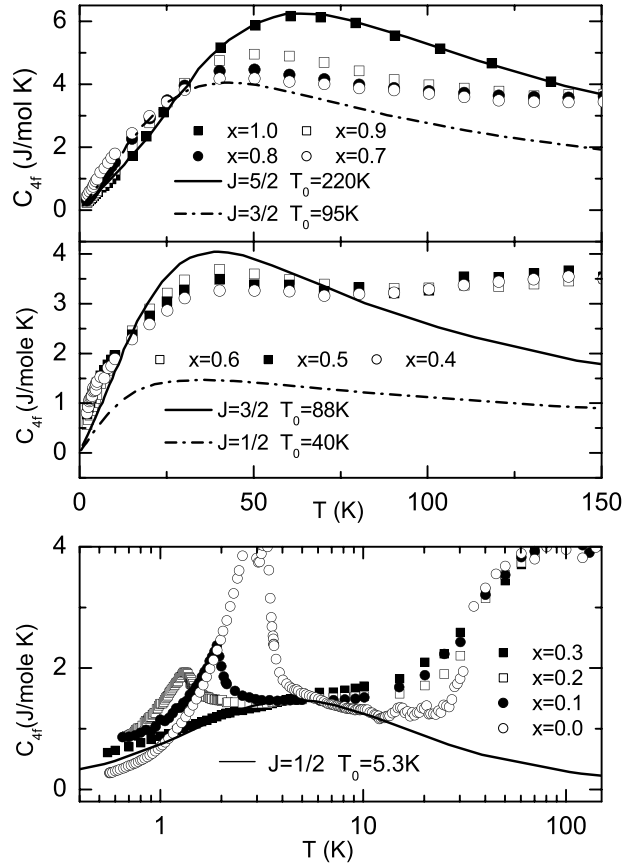


Figure 4. 4f-electron contribution to the specific heat, C_{4f} , given by the difference between the specific heats of $\text{LaNi}_{1-x}\text{Co}_x\text{Ge}_2$ and $\text{CeNi}_{1-x}\text{Co}_x\text{Ge}_2$. The solid curves indicate C_{4f} calculated from the Coqblin–Schrieffer model with various J values.

specific heat obtained from the $j = 1/2$ CS model (dashed curve), C_{Kondo} , and the Schottky anomaly with $E_1 = 90$ K and $E_2 = 480$ K (dotted curve), C_{CEF} , for $x = 0.5$, where E_1 and E_2 are the first and second excited doublets, respectively. The total specific heat (solid curve), $C_{\text{total}} = C_{\text{Kondo}} + C_{\text{CEF}}$, correctly describes the broad peak and the shoulder, but the absolute values are overestimated near the broad peak (40 K). For $x \leq 0.3$ (see the bottom panels of figure 5), the separate treatment for Kondo effects and CEF effects reproduces the data well with $E_1 = 150$ K and $E_2 = 530$ K. The Kondo temperature, T_K^{CS} , obtained from the analysis of the specific heat using the degenerate Kondo model mentioned just above is plotted in figure 6.

4. Discussion

Figure 7 shows the Co-concentration dependence of the dimensionless effective exchange coupling constant $N_F J_0$ that was calculated through $T_K = D \exp(-1/N_F J_0)$ [16], where T_K is the Kondo temperature evaluated by the analysis of specific heat. The prefactor D is related to the conduction-electron band width and is assumed to be constant (5×10^4 K) over the whole Co-concentration range. The effective coupling constant $N_F J_0$ is linearly proportional to x up to 0.6, sharply increases at $x = 0.6$, and increases with a relatively large slope for

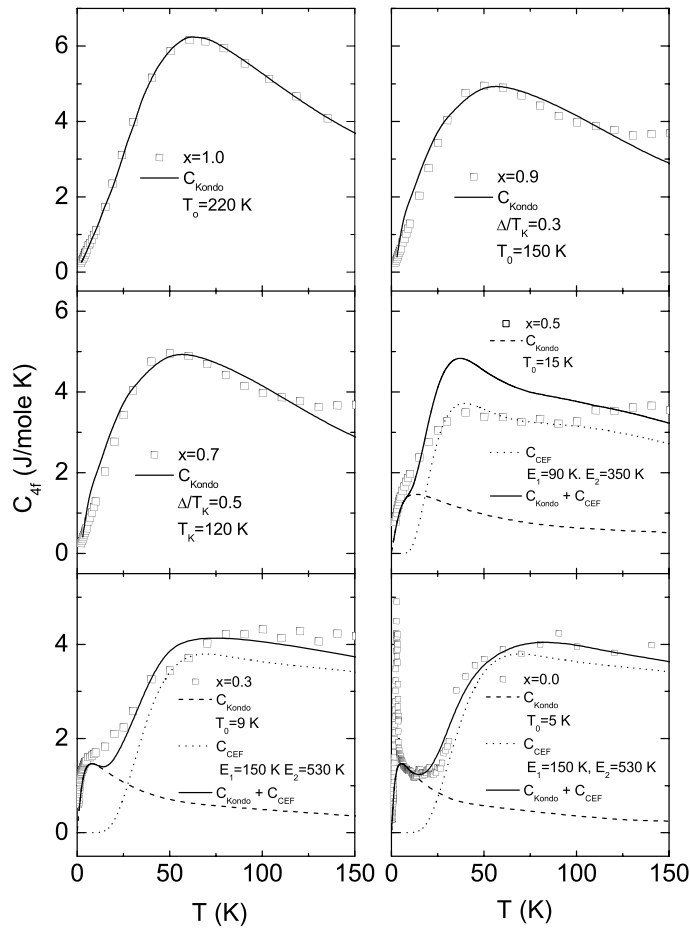


Figure 5. C_{4f} data of $\text{CeNi}_{1-x}\text{Co}_x\text{Ge}_2$ and the calculated results (solid curve) from the Coqblin–Schrieffer model in the presence of crystalline electric field. The details are mentioned in the text.

$x > 0.6$. Similar to Ce monopnictides (CeX), where p–f mixing increases the p holes [15], the doping dependence of $N_F J_0$ is most likely due to the hybridization between the Ce 4f and Co/Ni 3d electrons because the change in x is expected to affect only 3d bands near the Fermi level. For $\text{CeNi}_{1-x}\text{Co}_x\text{Ge}_2$, the lattice parameters are essentially independent of x , and thus the enhancement of hybridization with x most likely comes from a change in the electron density of states. To be more specific, Co substitution increases 3d electron states at the Fermi level because Co has one less 3d electron than Ni. Recently, reflectivity measurement has shown that the plasma edge in CeCoGe_2 is 5% higher than that in CeNiGe_2 [17], which is consistent with our proposition.

The sharp increase in $N_F J_0$ near 0.6 may be related to a change in the effective degeneracy number $N(= 2j + 1)$, i.e., $j = 1/2$ for $x \leq 0.6$ and $j = 3/2$ for $x > 0.6$. In CeSb [15], the p–f mixing of Ce 4f– Γ_8 (Γ_8 , the CEF excited state) with the Sb 5p state is sufficiently larger than that of Ce 4f– Γ_7 (Γ_7 , the ground state), leading to a decrease in the crystal field splitting between Γ_7 and Γ_8 . A similar analysis can be applied to $\text{CeNi}_{1-x}\text{Co}_x\text{Ge}_2$. Specific heat showed that the crystal field splitting tends to decrease with increasing x and sharply

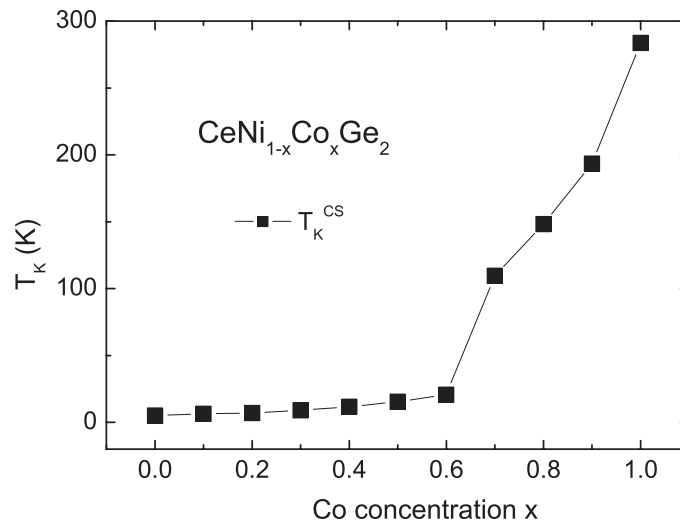


Figure 6. The Kondo temperature, T_K^{CS} , obtained from the analysis of the specific heat using the degenerate Kondo model mentioned in the text for $\text{CeNi}_{1-x}\text{Co}_x\text{Ge}_2$.

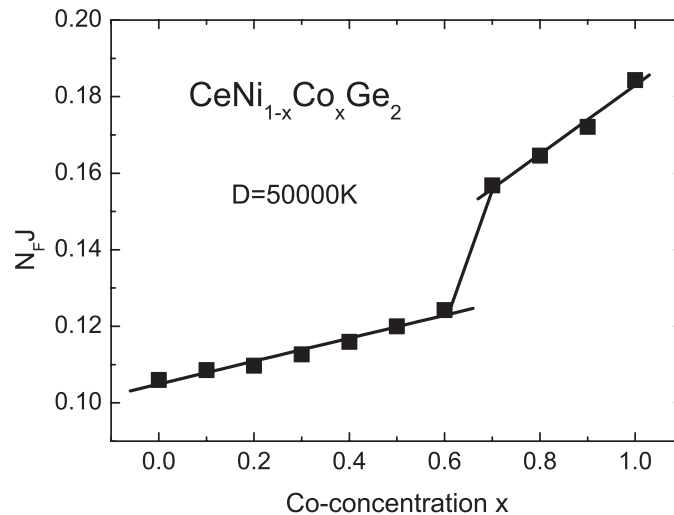


Figure 7. Dimensionless effective exchange coupling constant $N_F J_0$ estimated from the equation of $T_K = D \exp(-1/N_F J_0)$, assuming $D = 5 \times 10^4$ K.

decrease for $x \geq 0.6$, suggesting that the hybridization between the Ce 4f excited states and Co 3d states becomes dominant for larger x , leading to the steep increase in $N_F J_0$ at $x = 0.6$.

5. Conclusion

We have studied the various magnetic ground states that occurs from competition between the Kondo and RKKY energy scales for the heavy-fermion compounds of the alloying series $\text{CeNi}_{1-x}\text{Co}_x\text{Ge}_2$ in the whole concentration regime. The RKKY exchange dominates for $x < 0.3$, leading to local moment magnetism with negligible Kondo screening. With increasing

x , the antiferromagnetic transition temperature T_N is reduced and then becomes to zero at the critical concentration $x_c = 0.3$. A further increase of x stabilizes Fermi liquid behaviour. At the critical concentration, $C/T \propto -\log T$ are observed. The low temperature data of specific heat are well accounted for by the Kondo model for a degenerate impurity spin $J = 1/2$ ($x \leq 0.6$) and $5/2$ ($x \geq 0.9$) in the Coqblin–Schrieffer limit. At small x , the crystalline-electric-field (CEF) effect is negligible, while at high x the CEF effect is dominant. At intermediate x ($0.7 \leq x \leq 0.8$), the CEF energy scale is compensated with the Kondo energy scale, satisfying the Kondo model of $J = 3/2$.

Acknowledgments

This work is supported by the Korea Science and Engineering Foundation through the Center for Strongly Correlated Materials Research (CSCMR) at Seoul National University and by grant No. R01-2003-000-10095-0 from the Basic Research Programme of the Korea Science and Engineering Foundation.

References

- [1] Stewart G R 1984 *Rev. Mod. Phys.* **56** 755
- [2] Grewe N and Steglich F 1991 *Handbook on the Physics and Chemistry of Rare Earth* vol 14 (Amsterdam: Elsevier Science Publishers B. V.)
- [3] Doniach S 1977 *Physica B & C* **91** 231
- [4] Jung M H, Harrison N, Lacerda A H, Nakotte H, Pagliuso P G, Sarrao J L and Thompson J D 2002 *Phys. Rev. B* **66** 54420
- [5] Pecharsky V K and Gschneidner K A Jr 1991 *Phys. Rev. B* **43** 8238
- [6] Mun E D, Lee B K, Kwon Y S and Jung M H 2004 *Phys. Rev. B* **69** 85113
- [7] Moon E D, Hong S O, Kim D L, Ri H C and Kwon Y S 2003 *Physica B* **329–333** 516
- [8] Knebel G, Brando M, Hemberger J, Nicklas M, Trinkl W and Loidl A 1999 *Phys. Rev. B* **59** 12390
- [9] Sampathkumaran E V and Vijayaraghavan R 1986 *Phys. Rev. Lett.* **56** 2861
- [10] Pikul E A P, Kaczorowski D, Bukowski Z, Plackowski T and Gofryk K 2004 *J. Phys.: Condens. Matter* **16** 6119
- [11] Rosch A, Schröder A, Stockert O and Löhneysen H v 1997 *Phys. Rev. Lett.* **79** 159
- [12] Coqblin B and Schrieffer J R 1969 *Phys. Rev.* **185** 847
- [13] Desgranges H U and Rasul J W 1987 *Phys. Rev. B* **36** 328
- [14] Rajan V T 1983 *Phys. Rev. Lett.* **51** 308
- [15] Takahashi H and Kasuya T 1985 *J. Phys. C: Solid State Phys.* **18** 2709
Takahashi H and Kasuya T 1985 *J. Phys. C: Solid State Phys.* **18** 2721
- [16] Brandt N B and Moshchalkov V V 1984 *Adv. Phys.* **33** 373
Lawrence J 1979 *Phys. Rev. B* **20** 3770
- [17] Kimura S 2004 unpublished